
The Hamiltonian

Any theoretical description has to start with the definition of the system under consideration and a determination of the fundamental interactions present in the system. This information is all contained in the Hamiltonian which is the central quantity for any theoretical treatment. All physical and chemical properties of any system can be derived from its Hamiltonian. Since we are concerned with microscopic particles like electrons and atoms in surface science, the proper description is given by the laws of quantum mechanics. This requires the solution of the Schrödinger equation.

In this chapter we will first describe the Hamiltonian entering the Schrödinger equation appropriate for surface science problems. One general approximation that makes the solution of the full Schrödinger equation tractable is the decoupling of the electronic and nuclear motion which is called the Born–Oppenheimer or adiabatic approximation. We will then have a closer look at the specific form of the Hamiltonian describing surfaces. We will discuss the symmetries present at surfaces. Taking advantage of symmetries can greatly reduce the computational cost in theoretical treatments. Finally, we will introduce and illustrate the nomenclature to describe the structure of surfaces.

2.1 The Schrödinger Equation

In solid state physics as well as in chemistry, the only fundamental interaction we are concerned with is the electrostatic interaction. Furthermore, relativistic effects are usually negligible if only the valence electrons are considered. To start with, we treat core and valence electrons on the same footing and neglect any magnetic effects. Then a system of nuclei and electrons is described by the nonrelativistic Schrödinger equation with a Hamiltonian of a well-defined form,

$$H = T_{\text{nucl}} + T_{\text{el}} + V_{\text{nucl-nucl}} + V_{\text{nucl-el}} + V_{\text{el-el}}. \quad (2.1)$$

T_{nucl} and T_{el} are the kinetic energy of the nuclei and the electrons, respectively. The other terms describe the electrostatic interaction between the positively

charged nuclei and the electrons. As long as it is not necessary, we will not take the spin into account for the sake of clarity of the equations. Consequently, neglecting spin the single terms entering the Hamiltonian are explicitly given by

$$T_{\text{nucI}} = \sum_{I=1}^L \frac{\mathbf{P}_I^2}{2M_I}, \quad (2.2)$$

$$T_{\text{el}} = \sum_{i=1}^N \frac{\mathbf{p}_i^2}{2m}, \quad (2.3)$$

$$V_{\text{nucI-nucI}} = \frac{1}{2} \sum_{I \neq J} \frac{Z_I Z_J e^2}{|\mathbf{R}_I - \mathbf{R}_J|}, \quad (2.4)$$

$$V_{\text{nucI-el}} = - \sum_{i,I} \frac{Z_I e^2}{|\mathbf{r}_i - \mathbf{R}_I|}, \quad (2.5)$$

and

$$V_{\text{el-el}} = \frac{1}{2} \sum_{i \neq j} \frac{e^2}{|\mathbf{r}_i - \mathbf{r}_j|}. \quad (2.6)$$

Throughout this book we will use CGS-Gaussian units as it is common practice in theoretical physics textbooks. Atoms will usually be numbered by capital letter indices. Thus, Z_I stands for the charge of the I -th nuclei. The factor $\frac{1}{2}$ in the expressions for $V_{\text{nucI-nucI}}$ and $V_{\text{el-el}}$ ensures that the interaction between the same pair of particles is not counted twice.

In principle we could stop here because all what is left to do is to solve the many-body Schrödinger equation using the Hamiltonian (2.1)

$$H\Phi(\mathbf{R}, \mathbf{r}) = E\Phi(\mathbf{R}, \mathbf{r}). \quad (2.7)$$

The whole physical information except for the symmetry of the wave functions is contained in the Hamiltonian. In solving the Schrödinger equation (2.7), we just have to take into account the appropriate quantum statistics such as the Pauli principle for the electrons which are fermions. The nuclei are either bosons or fermions, but usually their symmetry does not play an important role in surface science. Often relativistic effects can also be neglected. Only if heavier elements with very localized wave functions for the core electron are considered, relativistic effects might be important since the localization leads to high kinetic energies of these electrons.

Note that only the kinetic and electrostatic energies are directly present in the Hamiltonian. We will later see that the proper consideration of the quantum statistics leads to contributions of the so-called *exchange-correlation energy* in the effective Hamiltonians. However, it is important to realize that the energy gain or cost according to additional effective terms has to be derived from the energy gain or cost in kinetic and electrostatic energy that is caused by the quantum statistics.

Unfortunately, the solution of the Schrödinger equation in closed form is not possible. Even approximative solutions are far from being trivial. In the rest of the book we will therefore be concerned with a hierarchy of approximations that will make possible the solution of (2.7) at least within reasonable accuracy. The first step in this hierarchy will be the so-called Born–Oppenheimer approximation.

2.2 Born–Oppenheimer Approximation

The central idea underlying the Born–Oppenheimer [1] or adiabatic approximation is the separation in the time scale of processes involving electrons and atoms. Except for hydrogen and helium, atoms have a mass that is 10^4 to 10^5 times larger than the mass of an electron. Consequently, at the same kinetic energy electrons are 10^2 to 10^3 times faster than the nuclei. Hence one supposes that the electrons follow the motion of the nuclei almost instantaneously. Most often one simply assumes that the electrons stay in their ground state for any configuration of the nuclei. The electron distribution then determines the potential in which the nuclei move.

In practice, one splits up the full Hamiltonian and defines the electronic Hamiltonian H_{el} for fixed nuclear coordinates $\{\mathbf{R}\}$ as follows

$$H_{\text{el}}(\{\mathbf{R}\}) = T_{\text{el}} + V_{\text{nucI-nucI}} + V_{\text{nucI-el}} + V_{\text{el-el}}. \quad (2.8)$$

In (2.8) the nuclear coordinates $\{\mathbf{R}\}$ do not act as variables but as parameters defining the electronic Hamiltonian. The Schrödinger equation for the electrons for a given fixed configuration of the nuclei is then

$$H_{\text{el}}(\{\mathbf{R}\})\Psi(\mathbf{r}, \{\mathbf{R}\}) = E_{\text{el}}(\{\mathbf{R}\})\Psi(\mathbf{r}, \{\mathbf{R}\}). \quad (2.9)$$

Again, in (2.9) the nuclear coordinates $\{\mathbf{R}\}$ are not meant to be variables but parameters. In the Born–Oppenheimer or adiabatic approximation the eigenenergy $E_{\text{el}}(\{\mathbf{R}\})$ of the electronic Schrödinger equation is taken to be the potential for the nuclear motion. $E_{\text{el}}(\{\mathbf{R}\})$ is therefore called the Born–Oppenheimer energy surface. The nuclei are assumed to move according to the atomic Schrödinger equation

$$\{T_{\text{nucI}} + E_{\text{el}}(\mathbf{R})\} A(\mathbf{R}) = E_{\text{nucI}} A(\mathbf{R}). \quad (2.10)$$

Often the quantum effects in the atomic motion are neglected and the classical equation of motion are solved for the atomic motion:

$$M_I \frac{\partial^2}{\partial t^2} \mathbf{R}_I = - \frac{\partial}{\partial \mathbf{R}_I} E_{\text{el}}(\{\mathbf{R}\}). \quad (2.11)$$

The force acting on the atoms can be conveniently evaluated using the Hellmann–Feynman theorem [2,3]

$$\mathbf{F}_I = -\frac{\partial}{\partial \mathbf{R}_I} E_{\text{el}}(\{\mathbf{R}\}) = \langle \Psi(\mathbf{r}, \{\mathbf{R}\}) | \frac{\partial}{\partial \mathbf{R}_I} H_{\text{el}}(\{\mathbf{R}\}) | \Psi(\mathbf{r}, \{\mathbf{R}\}) \rangle. \quad (2.12)$$

In principle, in the Born–Oppenheimer approximation electronic transitions due to the motion of the nuclei are neglected. One can work out the Born–Oppenheimer approximation in much more detail (see, e.g., [4]), however, what it comes down to is that the small parameter m/M is central for the validity of the adiabatic approximation (see Exercise 2.1). In fact, the Born–Oppenheimer approximation is very successful in the theoretical description of processes at surfaces. Still its true validity is hard to prove because it is very difficult to correctly describe processes that involve electronic transition (see Chap. 9).

If it takes a finite amount of energy to excite electronic states, i.e., if the adiabatic electronic states are well-separated, then it can be shown that electronically nonadiabatic transitions are rather improbable (see, e.g., [5]). In surface science this applies to insulator and semiconductor surfaces with a large band gap. At metal surfaces no fundamental band gap exists so that electronic transitions with arbitrarily small excitation energies can occur. Still, the strong coupling of the electronic states in the broad conduction band leads to short lifetimes of excited states and thus to a fast quenching of these states [6] so that their influence on surface processes is often limited.

On the other hand, there are very interesting processes in which electronic nonadiabatic processes are induced, as we will see in Chap. 9. The theoretical treatment of these systems requires special techniques that will also be discussed later in this book.

2.3 Structure of the Hamiltonian

Employing the Born–Oppenheimer approximation means first to solve the electronic structure problem for fixed atomic coordinates. The atomic positions determine the external electrostatic potential in which the electrons move. Furthermore, they determine the symmetry properties of the Hamiltonian.

Surface science studies are concerned with the structure and dynamics of surfaces and the interaction of atoms and molecules with surfaces. If not just ordered surface structures are considered, then the theoretical surface scientists has to deal with a system with only few degrees of freedom, the atom or molecule, interacting with a system, the surface or semi-infinite substrate, that has in principle an infinite number of degrees of freedom. Thus the substrate exhibits a quasi-continuum of states. One faces now the problem that usually different methods are used to treat the single subsystems: molecules are treated by quantum chemistry methods while surfaces are handled by solid-state methods.

To deal with both subsystems on an equal footing represents a real challenge for any theoretical treatment, but it also makes up the special attraction

of theoretical surface science. We will focus on this issue in more detail in the next chapter. But before considering a strategy to solve the Schrödinger equation it is always important to investigate the symmetries of the Hamiltonian. Not only rigorous results can be derived from symmetry considerations, but these considerations can also reduce the computational effort dramatically. This can be demonstrated very easily [7]. Let T be the operator of a symmetry transformation that leaves the Hamiltonian H invariant. Then H and T commute, i.e. $[H, T] = 0$. This means that according to a general theorem of quantum mechanics [8] the matrix elements $\langle \psi_i | H | \psi_j \rangle$ vanish, if $|\psi_i\rangle$ and $|\psi_j\rangle$ are eigenfunctions of T belonging to different eigenvalues $T_i \neq T_j$.

This property of the eigenfunctions can help us enormously in solving the Schrödinger equation. Imagine we want to determine the eigenvalues of a Hamiltonian by expanding the wave function in an appropriate basis set. Then we only need to expand the wave function within a certain class of functions having all the same eigenvalue with respect to a commuting symmetry operator. Functions having another symmetry will belong to a different eigenvalue. Since the numerical effort to solve the Schrödinger equation can scale very unfavorably with the number n of basis functions (up to n^7 for very accurate quantum chemical methods), any reduction in this number can mean a huge reduction in computer memory and time.

The mathematical tool to deal with symmetries is group theory. It is beyond the scope of this book to provide an introduction into group theory. There are many text books that can be used as a reference, for example [7, 9, 10]. I will rather describe the symmetries present at surfaces, which has also the important aspect of defining the terminology commonly used to specify surface structures. To set the stage, we will first start with ideal three-dimensional crystal structures.

A three-dimensional periodic crystal is given by an infinite array of identical cells. These cells are arranged according to the so-called Bravais lattice. It is given by all the position vectors of the form

$$\mathbf{R} = n_1 \mathbf{a}_1 + n_2 \mathbf{a}_2 + n_3 \mathbf{a}_3. \quad (2.13)$$

The \mathbf{a}_i are the three non-collinear unit vectors of the lattice, the n_i are integer numbers. The lattice vectors \mathbf{R} are not necessarily identical with atomic positions of the crystal, but in most cases they are indeed identified with atomic positions. In addition to the translational symmetry, there are also so-called point operations that transform the crystal into itself. Operations such as rotation, reflection and inversion belong to this point group. Furthermore, translations through a vector not belonging to the Bravais lattice and point operations can be combined to give additional distinct symmetry operations, such as screw axes or glide planes.

There are 14 different types of Bravais lattices in three dimensions. Now there can be more than one atom per unit cell of the Bravais lattice. Then the crystal structure is given as a Bravais lattice with a basis which corresponds to the positions of the additional atoms in the unit cell. If the lattice has a basis,

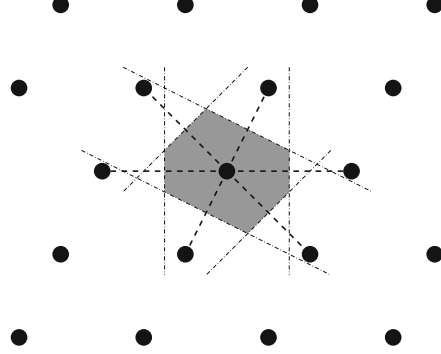


Fig. 2.1. Wigner–Seitz cell for a two-dimensional Bravais lattice. The six sides of the cell bisect the lines joining the central point to its six nearest neighbors. (After [11])

the symmetry of the corresponding crystal will usually be reduced compared to a crystal with just spherical symmetric atoms at the Bravais lattice sites. This enhances the number of symmetrically distinct lattices to in total 230. Details of these structure can be found in any text book of solid-state physics such as in [11, 12].

There is no way to uniquely choose the primitive unit cell of a Bravais lattice. Any cell that, when translated through all the Bravais lattice vectors, fills all space can serve as a unit cell. However, it is convenient to select a unit cell that has the full symmetry of the Bravais lattice. The so-called *Wigner–Seitz cell* has this property. It is defined as the region of space around a lattice point that is closer to that point than any other lattice point [11]. The construction of the Wigner–Seitz cell is demonstrated in Fig. 2.1 for a two-dimensional Bravais lattice. Select a lattice point and draw lines to the nearest neighbors. Then bisect each connection with a line and take the smallest polyeder that contains the points bounded by these lines. Note that in two dimensions the Wigner–Seitz cell is always a hexagon unless the lattice is rectangular (see Exercise 4.3).

The periodicity of a crystal lattice leads to the existence of a dual space that mathematically reflects the translational symmetry of a lattice. The dual space to the real space for periodic structures is called reciprocal space. The basis vectors are obtained from the basis vectors of the real space \mathbf{a}_i via

$$\mathbf{b}_1 = 2\pi \frac{\mathbf{a}_2 \times \mathbf{a}_3}{|\mathbf{a}_1 \cdot (\mathbf{a}_2 \times \mathbf{a}_3)|}. \quad (2.14)$$

The other two basis vectors of the reciprocal lattice \mathbf{b}_2 and \mathbf{b}_3 are obtained by a cyclic permutation of the indices in (2.14). By construction, the lattice vectors of the real space and the reciprocal space obey the relation

$$\mathbf{a}_i \cdot \mathbf{b}_j = 2\pi \delta_{ij}, \quad (2.15)$$

where δ_{ij} is the Kronecker symbol.

The reciprocal space is often called k -space since plane wave characterized by their wave vector \mathbf{k} are represented by single points in the reciprocal

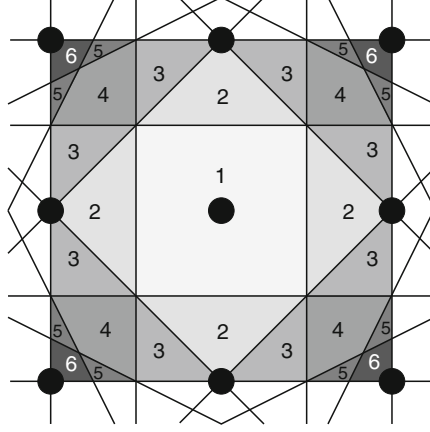


Fig. 2.2. Illustration of the definition of the Brillouin zones for a two-dimensional square reciprocal lattice. Note that only the first three Brillouin zones are entirely within the shaded areas. (After [11])

space. The eigenenergies of the electronic wave functions in periodic lattices are usually plotted as a function of their \mathbf{k} -vector in the *first Brillouin zone* which is defined as the Wigner–Seitz cell of the reciprocal lattice. As the name *first Brillouin zone* suggests, there are also higher-order Brillouin zones. Their construction is illustrated in Fig. 2.2 in two dimensions for a square reciprocal lattice. The n -th Brillouin zone is defined as the set of points that can be reached from the origin by crossing the $n - 1$ nearest bisecting planes. Note that each Brillouin zone is also a primitive unit cell of the reciprocal lattice. In fact, by translating the different sections of the higher-order Brillouin zones by appropriate reciprocal lattice vectors they can be rearranged to cover the first Brillouin zone. This can be easily checked for the second and third Brillouin zone in Fig. 2.2. In the periodic electronic structure theory this is called *backfolding*.

Reciprocal lattice vectors are used to denote lattice planes of the real-space lattice. Lattice planes of a Bravais lattice are described by the shortest reciprocal lattice vector $h\mathbf{b}_1 + k\mathbf{b}_2 + l\mathbf{b}_3$ that is perpendicular to this plane. The integer coefficients hkl are called *Miller indices*. Lattice planes are specified by the Miller indices in parentheses: (hkl) . Family of lattice planes, i.e. lattice planes that are equivalent by symmetry, are denoted by $\{hkl\}$. Finally, indices in square brackets $[hkl]$ indicate directions. For face-centered cubic (fcc) and body-centered cubic (bcc) crystals the Miller indices are usually related to the underlying simple cubic lattice, i.e., fcc and bcc crystals are described as simple cubic lattices with a basis.

For hcp crystals such as Ru, Co, Zn or Ti, the Miller index notation used to describe the orientation of lattice planes is slightly more complex since no standard Cartesian set of axes can be used. Instead the notation is based upon three axes at 120 degrees in the close-packed plane, and one axis (the c -axis) perpendicular to these planes. This leads to a four-digit index structure. However, since the first three axes are coplanar, the first three indices are not

independent but have to add up to zero. Hence the third index is redundant; in fact, it is sometimes omitted. For example, both Ru(001) and Ru(0001) describe the close-packed hexagonal plane of the hcp metal Ru.

The power of group theory to derive rigorous results can be nicely illustrated for periodic structures. The solution Ψ of the electronic Schrödinger equation (2.9) is a many-body wave function that incorporates the electron-electron interaction. However, as we will see below, there are many schemes to solve the electronic Schrödinger equation that involve the solution of effective one-particle Schrödinger equations of the form

$$\left\{ -\frac{\hbar^2}{2m} \nabla^2 + v_{\text{eff}}(\mathbf{r}) \right\} \psi_i(\mathbf{r}) = \varepsilon_i \psi_i(\mathbf{r}), \quad (2.16)$$

where the effective one-particle potential $v_{\text{eff}}(\mathbf{r})$ satisfies translational symmetry:

$$v_{\text{eff}}(\mathbf{r}) = v_{\text{eff}}(\mathbf{r} + \mathbf{R}), \quad (2.17)$$

with \mathbf{R} being any Bravais lattice vector.

The translational operations $T_{\mathbf{R}}$ form an Abelian group since the order of translations does not matter for the result of applying two successive translations. As mentioned above, the solutions of the Hamiltonian can be classified according to their symmetry properties. In group theory one says that solutions of different symmetries belong to so-called different representations of the symmetry group. Now there is an important theorem that the representations of an Abelian group are one-dimensional [7], which means that the eigenfunctions of the translational group can be written as

$$T_{\mathbf{R}} \psi_i(\mathbf{r}) = \psi_i(\mathbf{r} + \mathbf{R}) = c_i(\mathbf{R}) \psi_i(\mathbf{r}). \quad (2.18)$$

The eigenvalues $c_i(\mathbf{R})$ are complex numbers of modulus unity that have to satisfy

$$c_i(\mathbf{R}) c_i(\mathbf{R}') = c_i(\mathbf{R} + \mathbf{R}'), \quad (2.19)$$

which can be derived by applying two successive translation. From this relation it follows that the eigenvalues $c_i(\mathbf{R})$ are complex numbers of modulus one that can be expressed in an exponential form

$$c_i(\mathbf{R}) = e^{i\mathbf{k} \cdot \mathbf{R}}. \quad (2.20)$$

The eigenfunction $\psi_i(\mathbf{r})$ is thus characterized by the *crystal-momentum* \mathbf{k} that acts as a quantum number. Equation (2.18) can now be reformulated to state that the eigenstates of a periodic Hamiltonian can be written in the form

$$\psi_{\mathbf{k}}(\mathbf{r}) = e^{i\mathbf{k} \cdot \mathbf{r}} u_{\mathbf{k}}(\mathbf{r}) \quad (2.21)$$

with the periodic function

$$u_{\mathbf{k}}(\mathbf{r}) = u_{\mathbf{k}}(\mathbf{r} + \mathbf{R}) \quad (2.22)$$

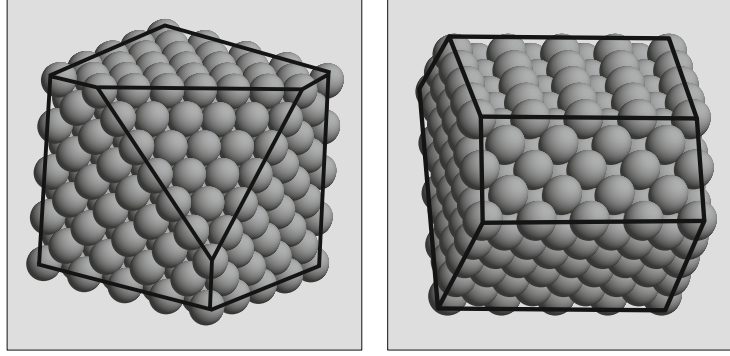


Fig. 2.3. Left panel: fcc crystal with 100 faces and one 111 face, right panel: fcc crystal with 100 faces and one 110 face

for all Bravais lattice vectors \mathbf{R} . This is the famous *Bloch theorem* which is an *exact* result since it is purely based on symmetry properties. Functions that obey the relation (2.21) are usually called *Bloch functions*.

A surface can be thought to be created by just cleaving an infinite crystal along one surface plane. A bulk-terminated surface, i.e. a surface whose configuration has not changed after cleavage, is called an *ideal* surface. Such ideal surfaces are shown in Fig. 2.3 where two fcc crystals are plotted that are terminated by the square $\{100\}$ faces. In addition, the cubes are further cleaved to indicate the other low-index faces of a face-centered cubic crystal. In the left panel of Fig. 2.3, the (111) face is shown which is perpendicular to the diagonal of the cubic unit cell. This (111) face with its hexagonal structure is the closest-packed fcc surface. In the right panel a (110) face is shown that is perpendicular to the diagonal of one of the square faces. The (110) surface has already a rather open structure with troughs running along the $[1\bar{1}0]$ direction.

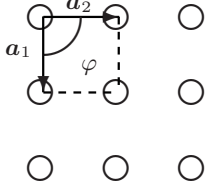
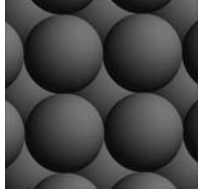
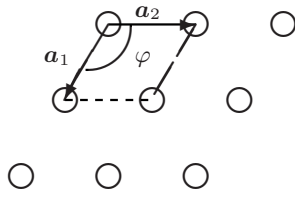
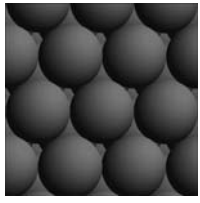
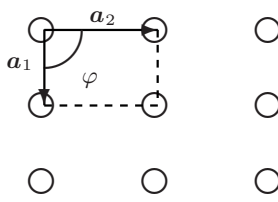
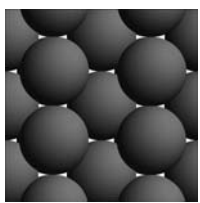
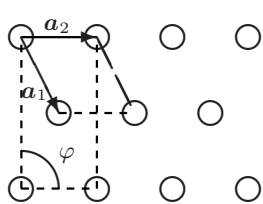
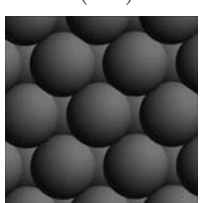
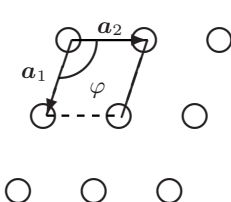
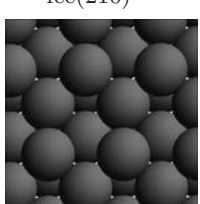
A semi-infinite solid with an ideal surface has no longer the three-dimensional periodicity of the crystal. Still there is a two-dimensional periodicity present parallel to the surface. In two dimensions, Bravais lattices can also be defined, equivalently to the three-dimensional case. Furthermore, there is also a two-dimensional Bloch theorem for a crystal having a periodic structure parallel to the surface which says that the electronic single-particle wave functions can be written as

$$\psi_{\mathbf{k}_{\parallel}}(\mathbf{r}) = e^{i\mathbf{k}_{\parallel} \cdot \mathbf{r}} u_{\mathbf{k}_{\parallel}}(\mathbf{r}), \quad (2.23)$$

where $u_{\mathbf{k}_{\parallel}}(\mathbf{r})$ has the two-dimensional periodicity of the surface.

There are five two-dimensional Bravais lattices which are sketched in Table 2.1. In fact, the centered rectangular lattice is just a special case of an oblique lattice, but it is usually listed separately. Examples of low-index planes of fcc and bcc crystals with the corresponding symmetry are also plotted. The

Table 2.1. The five two-dimensional Bravais lattices. In addition, examples of low-index planes of fcc and bcc crystal with the corresponding symmetry are plotted

2D lattice	Schematic sketch	Examples
Square $ \mathbf{a}_1 = \mathbf{a}_2 $ $\varphi = 90^\circ$		fcc(100) 
Hexagonal $ \mathbf{a}_1 = \mathbf{a}_2 $ $\varphi = 120^\circ$		fcc(111) 
Rectangular $ \mathbf{a}_1 \neq \mathbf{a}_2 $ $\varphi = 90^\circ$		fcc(110) 
Centered rectangular $ \mathbf{a}_1 \neq \mathbf{a}_2 $ $\varphi = 90^\circ$		bcc(110) 
Oblique $ \mathbf{a}_1 \neq \mathbf{a}_2 $ $\varphi \neq 90^\circ$		fcc(210) 

square (100) surface has a fourfold symmetry axis. The hexagonal (111) surface with its sixfold symmetry axis corresponding to the closest-packed surface is usually the most stable surface. Rectangular surfaces such as the (110) surface have already a more open structure. In fact, the low-index (100), (111) and (110) faces are the most often studied surfaces in surface science. Oblique surfaces are usually rather complex. Often they correspond to stepped surfaces like the example of the (210) surface that is shown in Table 2.1.

The planes plotted in Table 2.1 correspond to ideal surfaces where the interatomic distances are the same as in the bulk. However, at a real surface the fact that the bonding situation is entirely different compared to the bulk situation will cause a rearrangement of the atoms at and close to the surface. If this rearrangement preserves the symmetry of the bulk plane of termination, it is called *relaxation*. The corresponding surface structure is referred to as a (1×1) structure. However, if a significant restructuring of the surface occurs that changes the periodicity and symmetry of the surface, it is termed *reconstruction*.

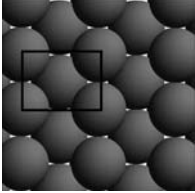
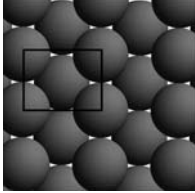
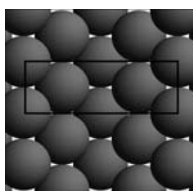
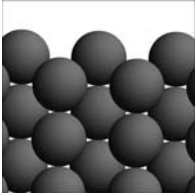
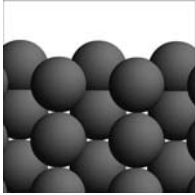
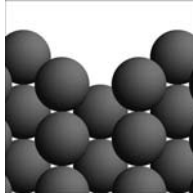
Such a structure is labeled with respect to the ideal termination of the corresponding surface plane. If the new surface unit cell is spanned by new vectors $\mathbf{a}_1^s = m\mathbf{a}_1$ and $\mathbf{a}_2^s = n\mathbf{a}_2$, the surface is labeled by $(hkl)(m \times n)$. Sometimes $(hkl)p(m \times n)$ is written, where p stands for *primitive*. Frequently, surface structures are observed with two atoms in the unit cell where the second atom occupies the centre of the unit cell. Such a situation is then labeled by $(hkl)c(m \times n)$, where c stands for *centered* [13].

The difference between relaxation and reconstruction is illustrated in Table 2.2 using the fcc(110) surface as an example. In the relaxed geometry just the distance between the top and the second layer is decreased with respect to the ideal surface. The top view of the relaxed structure indicates that the lateral symmetry of the surface remains unchanged. The last column of Table 2.2 presents a very prominent example for surface reconstructions, namely the so-called *missing-row reconstruction* which occurs for a number of materials such as Au(110) [14] or Pd(110). Every second row of the (110) surface running in $[1\bar{1}0]$ direction is missing. The surface unit cell becomes twice as large resulting in a 2×1 structure. Note that the microfacets forming the two ledges of the troughs correspond to close-packed triangular structures.

Semiconductor surfaces often show much more complex reconstruction patterns than metals. This is caused by the covalent nature of bonding in semiconductors where creating a surface strongly perturbs the bonding situation. The most famous example is the 7×7 reconstruction of the Si(111) surface. But also compound semiconductor such as GaAs exhibit extremely complex reconstruction patterns, as will be demonstrated in Sect. 4.3.

The periodicity of a surface can also be perturbed by the presence of adsorbates. For sufficiently strong adsorbate-substrate interactions commensurate adlayers will be created that result in larger surface unit cells as, e.g., for the $O(2 \times 2)/Pt(111)$ structure, where one fourth of the surface three-fold hollow sites are occupied by oxygen atoms. If the adsorbate-substrate interaction is

Table 2.2. Illustration of relaxation and reconstruction of the fcc(110) surface. In the relaxed structure just the distance between the top and the second layer is changed leaving the surface symmetry unchanged while in the (2×1) missing-row reconstruction every second row on the surface is missing

Structure	Ideal	Relaxed	Reconstructed
	1×1	1×1	2×1
Top view			
Side view			

weaker than the adsorbate-adsorbate coupling strength, as is often the case for organic adlayers, the adsorbate adlayer is not necessarily in registry with the surface resulting in an incommensurate adlayer for which no longer any surface periodicity can be expressed. This makes any theoretical treatment rather cumbersome.

A surface that is only slightly misaligned from a low index plane is called a *vicinal surface*. A vicinal surface is structured as a periodic array of terraces of a low-index orientation separated by monoatomic steps. In Fig. 2.4, a (911) surface is shown illustrating the structure of a vicinal surface. The high-index (911) surface consists of 5 atomic rows of (100) orientation separated by a step with a (111) ledge, i.e., the ledge represents (111) microfacets. In fact, in order to make the structure of vicinal surfaces immediately obvious, they are often denoted by $n(hkl) \times (h'k'l')$ where (hkl) and $(h'k'l')$ are the Miller indices of the terraces and of the ledges, and n gives the width of the terraces in numbers of atomic rows parallel to the ledges. By studying vicinal surfaces, the influence of steps on, e.g., adsorption properties or reactions on surfaces can be studied in a well-defined way. Further defects that can exist on surfaces are kinks, adatoms, vacancies and adatom islands. These defects are illustrated in

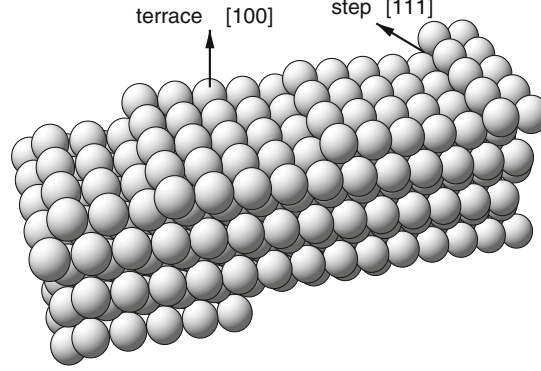


Fig. 2.4. A stepped $(911) = 5(100) \times (111)$ vicinal surface. Steps with ledges of (111) orientations separate (100) terraces that are 5 atom rows wide

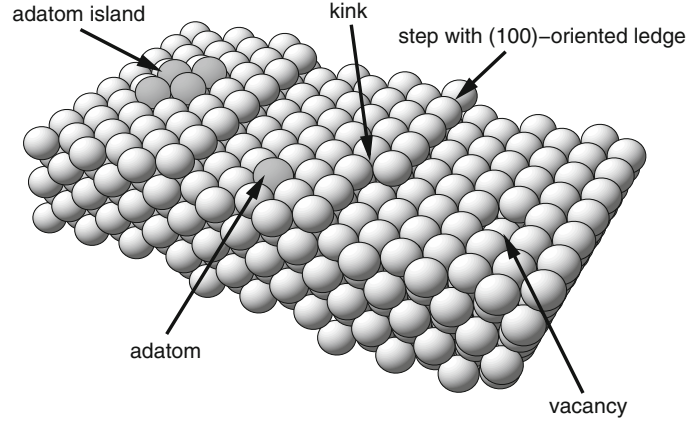


Fig. 2.5. Illustration of defects on surfaces such as steps, kinks, adatoms, adatom islands, and vacancies

Fig. 2.5. In fact, the plotted surface corresponds to a defected $(755) = 5(111) \times (100)$ surface where the steps are made of (100) -oriented microfacets. The creation of defects is usually associated with a cost of energy. Yet, at non-zero surface temperature there will always be a certain amount of defects present because of entropic reasons. This is a particular problem for experimentalists who have to check whether their observed results on nominally flat surfaces might be dominated by minority defect sites.

On the other hand, the study of defects is important because often the defects are considered to be the active sites for surface reactions. This is relevant for the understanding of, for example, real catalysts which usually exhibit a very defect-rich structure. Furthermore, the defects depicted in Fig. 2.5 all appear during growth processes on surfaces. Thus the properties are relevant for a true understanding of growth, as will be shown in Sect. 8.5.

Exercises

2.1 Born–Oppenheimer Approximation

Expand the eigenfunctions of the total Hamiltonian

$$H = T_{\text{nuc}} + T_{\text{el}} + V_{\text{nuc} - \text{nuc}} + V_{\text{nuc} - \text{el}} + V_{\text{el} - \text{el}} \quad (2.24)$$

according to

$$\Phi(\mathbf{R}, \mathbf{r}) = \sum_{\mu} A_{\mu}(\mathbf{R}) \Psi_{\mu}(\mathbf{r}, \mathbf{R}), \quad (2.25)$$

where the $\Psi_{\mu}(\mathbf{r}, \mathbf{R})$ are the eigenfunctions of the electronic Hamiltonian

$$H_{\text{el}}(\{\mathbf{R}\}) = T_{\text{el}} + V_{\text{nuc} - \text{nuc}} + V_{\text{nuc} - \text{el}} + V_{\text{el} - \text{el}}. \quad (2.26)$$

By multiplying the many-body Schrödinger equation (2.7) by $\langle \Psi_{\nu} |$, a set of coupled differential equations for the nuclear wave functions $A_{\mu}(\mathbf{R})$ can be obtained.

- a) Write down the coupled equations for the nuclear wave functions $A_{\mu}(\mathbf{R})$. Which terms are neglected in the Born–Oppenheimer approximation (compare with (2.10))?
- b) Discuss the meaning of the neglected terms. Give an estimate for the terms that are diagonal in the electronic wave functions.

2.2 Surface Structures

- a) Determine the structure and the reciprocal lattice of the (100), (110) and (111) unreconstructed surfaces of bcc and fcc crystals. Give the basis vectors of the corresponding unit cells in units of the bulk cubic lattice constant a .
- b) Find the surface first Brillouin zone for each surface.

2.3 Wigner–Seitz Cell in Two Dimensions

Consider a Bravais lattice in two dimensions.

- a) Prove that the Wigner–Seitz cell is a primitive unit cell.
- b) Show that the Wigner–Seitz cell for any two-dimensional Bravais lattice is either a hexagon or a rectangle.

2.4 Reciprocal Lattice

- a) Show that the reciprocal lattice belongs to the same symmetry group as the underlying Bravais lattice in real space.
- b) Determine the reciprocal lattices and the first Brillouin zones of all the two-dimensional Bravais lattices shown in Table 2.1.

2.5 Lattice Spacing and Vicinal Surfaces

Consider a lattice plane in a three-dimensional crystal described by the Miller indices (hkl) .

a) Show that the reciprocal lattice vector $\mathbf{G} = h\mathbf{b}_1 + k\mathbf{b}_2 + l\mathbf{b}_3$ is perpendicular to this plane.

b) Show that the distance between two adjacent (hkl) planes is given by

$$d_{hkl} = \frac{2\pi}{|\mathbf{G}|}$$

c) Consider the unreconstructed $(11n)$ surface of a fcc crystal with cubic lattice constant a and n an odd number. This surface consists of (001) terraces terminated by steps of $[\bar{1}10]$ orientation. Show that the terraces have a width of $a \times n/\sqrt{8}$ and that the interlayer distance is given by $a/\sqrt{n^2 + 2}$. Prove that the miscut angle between $(11n)$ and (001) surfaces is $\arctan(\sqrt{2}/n)$.

d) The unreconstructed $(10n)$ surface of a fcc crystal with cubic lattice constant a also consists of (001) terraces terminated by monoatomic steps. Determine the terrace width, the lattice distance between adjacent $(10n)$ planes and the miscut angle to the (001) plane.



<http://www.springer.com/978-3-540-68966-9>

Theoretical Surface Science

A Microscopic Perspective

Groß, A.

2009, XIII, 342 p., Hardcover

ISBN: 978-3-540-68966-9